

Combining crystallogenesi s methods to produce diffraction-quality crystals of a psychrophilic tRNA-maturation enzyme

Raphaël de Wijn,^a Oliver Hennig,^b Felix G. M. Ernst,^b Bernard Lorber,^a Heike Betat,^b Mario Mörl^b and Claude Sauter^{a*}

Received 31 August 2018

Accepted 16 October 2018

Edited by R. Sankaranarayanan, Centre for Cellular and Molecular Biology, Hyderabad, India

Keywords: microseeding; counter-diffusion; trace fluorescent labeling; optimization; crystallogenesi s; tRNA maturation; CCA-adding enzyme; *Planococcus halocryophilus*.

^aArchitecture et Réactivité de l'ARN, UPR 9002, Université de Strasbourg, IBMC, CNRS, 15 Rue R. Descartes, 67084 Strasbourg, France, and ^bInstitute for Biochemistry, Leipzig University, Brüderstrasse 34, 04103 Leipzig, Germany.

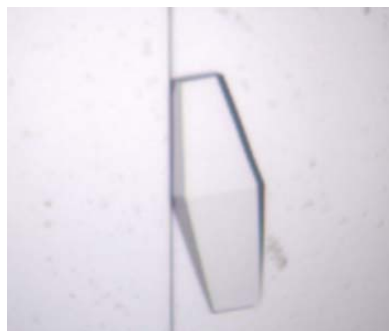
*Correspondence e-mail: c.sauter@ibmc-cnrs.unistra.fr

The determination of conditions for the reproducible growth of well diffracting crystals is a critical step in every biocrystallographic study. On the occasion of a new structural biology project, several advanced crystallogenesi s approaches were tested in order to increase the success rate of crystallization. These methods included screening by microseed matrix screening, optimization by counter-diffusion and crystal detection by trace fluorescent labeling, and are easily accessible to any laboratory. Their combination proved to be particularly efficient in the case of the target, a 48 kDa CCA-adding enzyme from the psychrophilic bacterium *Planococcus halocryophilus*. A workflow summarizes the overall strategy, which led to the production of crystals that diffracted to better than 2 Å resolution and may be of general interest for a variety of applications.

1. Introduction

The search for crystallization conditions for a new biomolecule is often sample-consuming and time-consuming. This critical step generally consists of a trial-and-error process and the screening of thousands of solvent conditions. However, it has been shown that expanding the set of crystallization trials beyond a few hundred does not significantly increase the number of useful hits (Newman *et al.*, 2005; Newman, 2011). Instead, using alternative approaches that provide a better sampling of the supersaturation landscape, such as counter-diffusion (CD; Otálora *et al.*, 2009), that facilitate nucleation, such as microseeding (Bergfors, 2003; D'Arcy *et al.*, 2007; D'Arcy *et al.*, 2014), or that help to detect positive results, such as trace fluorescent labeling (TFL; Pusey *et al.*, 2015), may dramatically improve the output of the screening process. In this work focused on tRNA-maturation enzymes, we combined conventional screening with more advanced although easy-to-implement crystallogenesi s methods to accelerate the definition of crystallization conditions for a new CCA-adding enzyme.

CCA-adding enzymes are ubiquitous nucleotidyltransferases that are involved in the post-transcriptional maturation of transfer RNAs (tRNAs) and belong to the polymerase β superfamily (Betat *et al.*, 2010). They add two cytosine nucleotides and one adenine nucleotide at the 3' end of tRNA to synthesize and maintain this specific CCA sequence, which represents a highly conserved site for tRNA aminoacylation



© 2018 International Union of Crystallography

Table 1
Macromolecule-production information.

Source organism	<i>P. halocryophilus</i>
Expression vector	pET-30 Ek/LIC
Expression host	<i>E. coli</i> BL21 (DE3)
Complete amino-acid sequence of the construct†	MHHHHHSSGLVPRGSGMKETA AAKFER QHMDSPDLGTD DDDD KMNTAIKVIHTL KAAGFEAYIVGGAVRDLLLGKTPHDV DVASSALPQQVKVLFDR TVD TGIDHG TVLVLLDGEIEV TT FRTESSYSDNR RPDSVEFVLSLEEDLRR R DFTINAMA MTEDLKIIDPF GG KEDLNK N VIRAVG DPDERFEEDALRMLRAIR F SGQLDFI IDMKTLLSIRRHARLIR F IAVERLKS EIDKIFVNP SM QKSMAYLK D SVL TR F LPVGGLEF EV DWITYHTDGN PT Y GW LY LLHQQRQ FT DIKDYR F SNEEKRLIE K S LELTALNTWDQ W TFYKY T LKQLEM ASRV T GKKKDLAAIKR Q LP I QSRSEL AVD G WDLIEWSGAKSGP W LK V WIEKI ERLIVY G ILKNDKELIK D WFEDEYHS HT
No. of amino acids	420
Molecular mass (Da)	48423
Abs 0.1%‡ at 280 nm ($M^{-1} \text{ cm}^{-1}$)	1.36

† The purification tag, including 6×His, is underlined. ‡ Equal to a 1 g l⁻¹ solution.

by cognate aminoacyl-tRNA synthetases. This polymerization activity is performed without any DNA or RNA template, but is exclusively controlled by a set of highly conserved amino-acid residues and specific movements in the single nucleotide-binding pocket (Li *et al.*, 2002; Neuenfeldt *et al.*, 2008; Ernst *et al.*, 2015). During the switch between cytosine triphosphate (CTP) and adenosine triphosphate (ATP) specificity, motion affects not only the amino acids near the catalytic center, but also the global structure and organization of the enzyme (Tomita *et al.*, 2006). The present work was initiated to examine the situation in psychrophilic organisms that thrive in the cold and produce proteins with enhanced structural flexibility (De Maayer *et al.*, 2014). Therefore, unlike their thermophilic homologs, which are known to be rigid and stable, psychrophilic enzymes constitute more challenging targets for crystallization (Bae & Phillips, 2004). To study the cold-adaptation of CCA-adding enzymes, we selected the protein from *Planococcus halocryophilus* (*PhaCCA*), a bacterium that lives in the Arctic permafrost (Mykytczuk *et al.*, 2012). In this article, we describe the crystallogensis strategy which enabled us to rapidly and efficiently define growth conditions for crystals that diffracted to high resolution, paving the way for the structure determination of a psychrophilic CCA-adding enzyme.

2. Materials and methods

2.1. Macromolecule production and fluorescent labeling

The CCA-adding enzyme from *P. halocryophilus* (*PhaCCA*) was produced as described by Ernst *et al.* (2018). Briefly, it was overproduced in *Escherichia coli* BL21 (DE3) cca:cam cells lacking the endogenous CCA-adding enzyme. Gene expression was induced with IPTG and *PhaCCA* was purified by affinity chromatography and size-exclusion chromatography

(SEC) using HisTrap FF and Superdex 75 columns (GE Healthcare), respectively. After SEC, fractions containing the enzyme were pooled and concentrated using a 3 ml Slide-A-Lyzer cassette (3.5 kDa molecular-weight cutoff; Thermo Fisher Scientific) embedded in PEG 20 000 (Roth) to a final concentration of 4 to 5 mg ml⁻¹ (depending on the batch). The purified enzyme was stored at 277 K in 50 mM Tris-HCl pH 7.5, 200 mM NaCl, 5 mM MgCl₂. Its homogeneity at 293 K was verified by SEC using a Bio SEC-3 150 column (Agilent) on an Agilent 1200 ChemStation HPLC system and by dynamic light scattering (DLS) using a Zetasizer Nano ZS instrument (Malvern) and a 20 µl quartz cuvette (Fig. 1). The protein concentration was determined using a NanoDrop ND-1000 spectrophotometer. Macromolecule-production information is summarized in Table 1.

In order to facilitate the detection of protein crystals, *PhaCCA* was fluorescently labeled with carboxyrhodamine succinimidyl ester (Invitrogen; catalog No. C6157). Protein labeling was performed with 80 µl of enzyme solution at 5 mg ml⁻¹ (close to the maximum solubility in the storage buffer). The labeled solution was not mixed back with the protein stock solution but kept separately at 277 K. It will be referred to as *PhaCCA*-TFL. Other steps of the TFL were as described by Pusey *et al.* (2015).

2.2. Crystallization

2.2.1. Initial screening by vapor diffusion. All experiments were performed at 293 K. Prior to crystallization assays, *PhaCCA* was ultracentrifuged at 105 000g and 277 K for 1 h in a Sorvall Discovery M150 SE ultracentrifuge (Hitachi). Initial screens, microseed matrix screening and further optimizations were carried out by vapor diffusion using a Mosquito Crystal pipetting robot (TTP Labtech, UK) and 96-well sitting-drop plates (CrystalQuick plate, three round subwells; Greiner Bio-One). Initial screens were performed using the commercial kits Index (Hampton Research) and JBScreen JCSG++ (Jena Bioscience). Drops were prepared by mixing 300 or 150 nl *PhaCCA* at 4.5 mg ml⁻¹ in storage buffer with 150 nl of the kit solution and were equilibrated against 50 µl reservoir solution. Duplicates were stored at either 277 or 293 K.

2.2.2. Optimization by counter-diffusion (CD). Initial hits obtained in ammonium sulfate were optimized using a CD kit (Triana Science & Technologies, Spain) consisting of six solutions of this salt at a pH ranging from 4 to 9. Capillaries (length 50 mm, inner diameter 0.2 mm) were filled with protein solution, sealed at one extremity with plasticine and plunged into Granada Crystallization Box-Dominos (GCB-D; Triana Science & Technologies) containing individual kit solutions. CD experiments were performed at 293 K. The section of the capillary containing the largest crystals was cut, sealed with plasticine, mounted on a standard goniometer base and cryocooled in liquid nitrogen.

2.2.3. Seed-stock preparation. To perform microseed matrix screening (MMS; D'Arcy *et al.*, 2007, 2014), small crystals grown by counter-diffusion (see above) with a solution consisting of 3 M ammonium sulfate, 0.1 M sodium acetate

pH 5 were recovered from the capillaries, crushed with Seed Beads (Hampton Research), vortexed and diluted in 50 μl of the same crystallant solution. This suspension was stored at 277 K and is referred to as the 'seed stock'.

2.2.4. Microseed matrix screening and optimization by vapor diffusion. For easy crystal detection in subsequent experiments, 22.5 μl *PhaCCA* at 5 mg ml⁻¹ was added to 0.5 μl *PhaCCA*-TFL at 1.3 mg ml⁻¹ (corresponding to a 0.6% contamination with TFL protein) and 7.5 μl seed-stock solution just before dispensing with the Mosquito robot. MMS was performed with JBScreen JCSG++ at 293 K by mixing 200 nl macromolecule solution (native and TFL enzyme plus seeds) with 140 nl crystallant solution. For further optimization, plates were set up with drops with the same mixing ratio against a reservoir containing 50 μl of the selected conditions (Table 2). Crystallization drops were observed with a Zeiss Scope A1 (Explora Nova) and TFL was revealed under illumination provided by an XtalLight 100C (Xtal Concepts).

2.3. Data collection and processing

Prior to cryocooling, the crystals grown by vapor diffusion were soaked in cryoprotectant solutions. For crystals grown in conditions A8 and B12 (see Table 2) containing PEG 3350, the crystallant concentration was increased to 25% (*m/v*); for those in condition E8 20% (*m/v*) glycerol was added to the condition. Crystals were soaked for 30 s in their respective cryoprotectant solution, fished out with cryomounts (MiTeGen) and plunged into liquid nitrogen. Crystals grown by CD were directly cryocooled inside the capillaries. Diffraction data were collected on beamline X06DA at the Swiss Light Source, Villigen, Switzerland or on the PROXIMA-1 beamline at

Synchrotron SOLEIL, Saint-Aubin, France, which were equipped with PILATUS 2M and 6M detectors, respectively. All data sets were processed with *XDS* (Kabsch, 2010) and data-collection statistics are summarized in Table 3. Molecular replacement (MR) was performed with *Phaser* and the *PHENIX* package (McCoy *et al.*, 2007; Adams *et al.*, 2010) using data collected from a crystal grown by CD in capillaries and PDB entry 1miv (Li *et al.*, 2002; sequence identity 38%), corresponding to the CCA-adding enzyme from *Geobacillus stearothermophilus*, as a search model.

3. Results and discussion

The CCA-adding enzyme from *P. halocryophilus* over-produced in *E. coli* was purified by two chromatographic steps. Quality control of the purified protein by analytical SEC and DLS confirmed its homogeneity, monodispersity and stability in solution, with a single population with a mean diameter of 9.2 nm and a polydispersity index of 0.08% (Fig. 1). The initial crystallization performed with two commercial kits, both at 277 and 293 K, and *PhaCCA* at 4.5 mg ml⁻¹ yielded small crystals in seven conditions (A4, A9, C6, B5 and C11 from Index and E2 and H2 from JBScreen JCSG++) at 293 K using a 2:1 ratio of protein:crystallant solution (Fig. 2, top). Three of these hits yielded crystals that produced diffraction patterns with reflections to between 5 and 10 Å resolution. Ammonium sulfate was a common feature of five of the hits and of two of the diffracting crystals. This encouraged us to carry out optimization assays by CD with this crystallant at various pH values. This crystallization method samples the supersaturation space through the creation of extended concentration gradients by diffusion of the crystallant inside

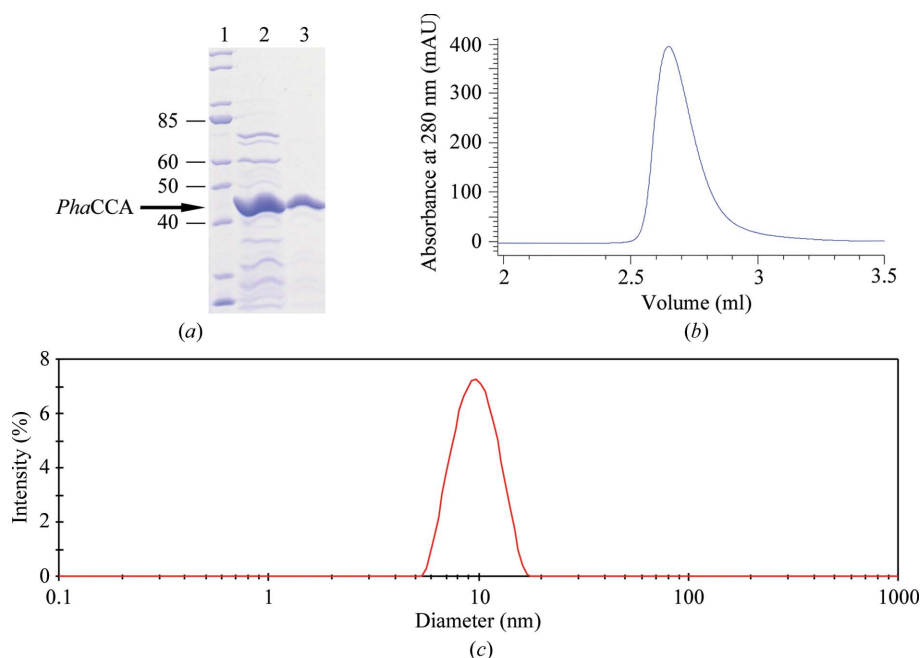


Figure 1

Quality control of *PhaCCA* prior to crystallization. (a) Denaturing SDS-PAGE gel showing the purity of the sample at different steps of the purification process. Lane 1, molecular-mass ladder (labeled in kDa); lane 2, after elution from the HisTrap column; lane 3, after elution from the SEC column. The sample homogeneity was assessed by analytical SEC (b) and DLS (c).

Table 2
Crystallization conditions for *PhaCCA*.

Method	Counter-diffusion	Vapor diffusion
Container	Glass capillary in GCB-Domino	CrystalQuick plate
Temperature (K)	293	293
Protein concentration (mg ml ⁻¹)	4.5	5
Composition of protein buffer solution	50 mM Tris-HCl pH 7.5, 200 mM NaCl, 5 mM MgCl ₂	50 mM Tris-HCl pH 7.5, 200 mM NaCl, 5 mM MgCl ₂
Composition of crystallant solution	3 M ammonium sulfate, 100 mM sodium acetate pH 5	A8: 20% (m/v) PEG 3350, 200 mM lithium sulfate pH 6.6 B12: 20% (m/v) PEG 3350, 200 mM potassium citrate pH 8.3 E8: 100 mM sodium acetate, 1 M diammonium hydrogen phosphate pH 4.5
Volume of sample	1.5 µl	200 nl
Volume of reservoir	1 ml	50 µl

Table 3
Data collection and processing.

Values in parentheses are for the outer shell.

Crystal source	Counter-diffusion	Vapor diffusion		
		Condition A8	Condition B12	Condition E8
Diffraction source	X06DA, SLS	PROXIMA-1, SOLEIL	PROXIMA-1, SOLEIL	PROXIMA-1, SOLEIL
Wavelength (Å)	1.000	0.978	0.978	0.978
Temperature (K)	100	100	100	100
Detector	PILATUS 2M	PILATUS 6M	PILATUS 6M	PILATUS 6M
Crystal-to-detector distance (mm)	350	320	320	320
Rotation range per image (°)	0.2	0.1	0.1	0.1
Total rotation range (°)	360	180	180	180
Exposure time per image (s)	0.2	0.1	0.1	0.1
Space group	<i>P</i> 4 ₃ 2 ₁ 2			
<i>a</i> , <i>b</i> , <i>c</i> (Å)	70.0, 70.0, 292.5	69.7, 69.7, 290.9	69.8, 69.8, 291.6	69.4, 69.4, 290.9
α , β , γ (°)	90, 90, 90	90, 90, 90	90, 90, 90	90, 90, 90
Mosaicity (°)	0.19	0.06	0.07	0.04
Resolution range (Å)	50–2.70 (2.87–2.70)	50–1.85 (1.96–1.85)	50–2.09 (2.22–2.09)	50–1.80 (1.91–1.80)
Total No. of reflections	481011 (78334)	812446 (127833)	467767 (71156)	890444 (139573)
No. of unique reflections	19869 (3210)	62686 (9806)	43652 (6782)	68555 (10787)
Completeness (%)	94.4 (97.9)	99.8 (98.7)	99.7 (98.2)	99.9 (99.3)
Multiplicity	24.2 (24.4)	13.0 (13.0)	10.7 (10.5)	13.0 (12.9)
$\langle I/\sigma(I) \rangle^\dagger$	13.9 (1.7)	18.1 (0.9)	12.0 (0.75)	19.5 (0.7)
R_{meas}^\ddagger (%)	29.5 (217.8)	9.2 (223.2)	12.4 (264.7)	7.4 (264.8)
CC _{1/2} [†] (%)	99.7 (65.2)	100 (51.0)	99.9 (49.6)	100 (59.0)
Overall <i>B</i> factor from Wilson plot (Å ²)	55.9	43.6	56.0	44.8
Solvent content (%)	66.7	66.6	66.7	66.6

[†] Data with low $I/\sigma(I)$ in the outer shell (<2.0) were included based on the CC_{1/2} criterion (correlation between two random halves of the data set of $>50\%$) as proposed by Karplus & Diederichs (2012). [‡] Redundancy-independent $R_{\text{meas}} = \sum_{hkl} \{N(hkl)/[N(hkl) - 1]\}^{1/2} \sum_i |I_i(hkl) - \langle I(hkl) \rangle| / \sum_{hkl} \sum_i I_i(hkl)$, where $N(hkl)$ is the data multiplicity.

capillaries. Crystals with a round-shaped habit were observed after two weeks at pH values from 4 to 8, except at pH 5 where they grew as well faceted bipyramids (Fig. 2). X-ray analysis of one of these crystals led to a first data set to 2.7 Å resolution (first column in Table 3). This tetragonal crystal form was characterized by an elongated unit cell ($a = b = 70$, $c = 290$ Å), a single protein molecule in the asymmetric unit and a high solvent content (67%). A clear molecular-replacement solution was found in space group *P*4₃2₁2 with *Phaser* (LLG score of 158) using a polyalanine version of the *G. stearothermophilus* enzyme (PDB entry 1miv) as a starting model.

To increase the diffraction limit of the crystals and/or find new crystallization conditions, MMS was performed using crushed crystals extracted from CD capillaries. A single screen of 96 conditions (JBScreen JCSG++, Jena Bioscience) was set up with and without seeds. The use of MMS drastically increased the number of hits obtained by vapor diffusion: a total of 34 hits were obtained after 4 d with seeds, compared

with a single hit after several months without seeds (Fig. 2). The latter condition (H2 from JBScreen JCSG++) was also found by MMS and in the initial screening. It cannot be excluded that the ammonium sulfate present in the seed stock had a positive effect on the screening result. However, a seed stock prepared from one of the new conditions (E8 from JBScreen JCSG++), which did not contain this salt, was found to be equally effective in optimization, suggesting that the effect was at least partially owing to the microcrystals.

Fluorescent protein labeling with carboxyrhodamine succinimidyl ester facilitated discrimination between protein and salt crystals (owing to the high salt concentration in the seed stock, MMS generated many salt crystals). Although the protein contains nine tryptophan residues, TFL led to a much brighter fluorescent signal than intrinsic tryptophan fluorescence under UV light. It did not perturb crystallization and provided a clear identification of the *PhaCCA* crystals, as presented in Fig. 3. Nucleation is generally the limiting event

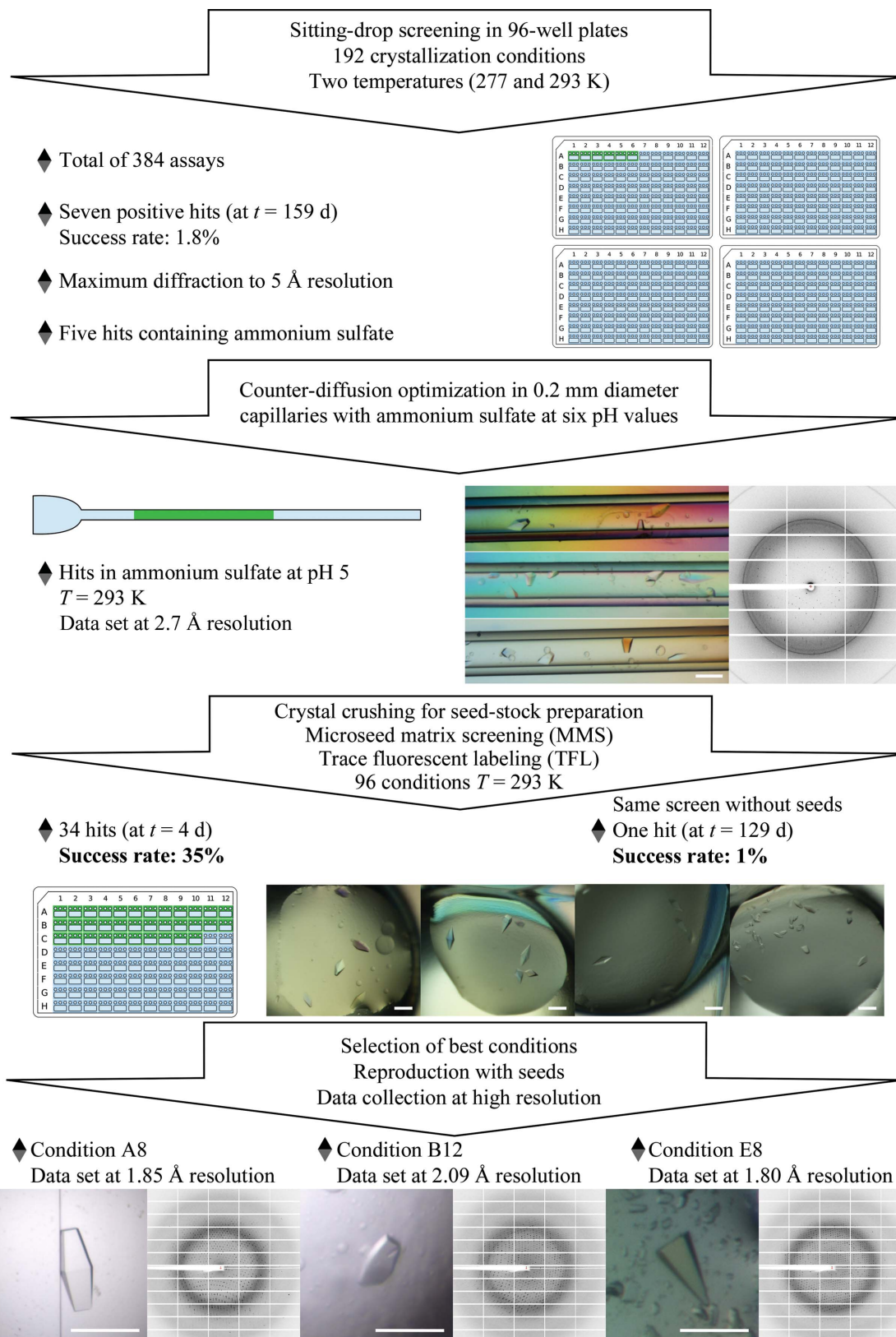


Figure 2

Workflow of the crystallogenesis strategy for *PhaCCA*. The color photograph in the center displays bipyramidal crystals that grown in three contiguous regions of a CD capillary. The other photographs in color show crystals grown in drops equilibrated by vapor diffusion. The scale bars on the crystal micrographs are 0.2 mm in length.

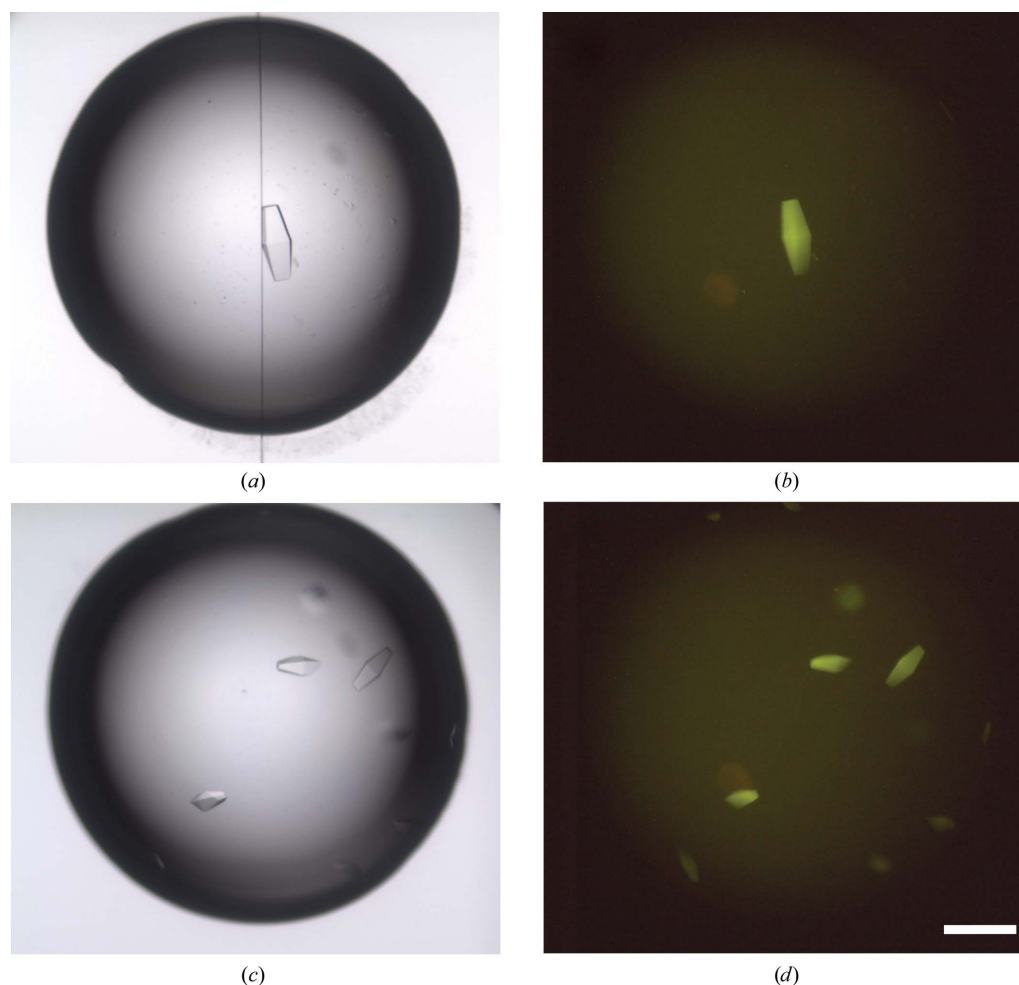


Figure 3 Detection of *PhaCCA* crystals by TFL. Crystals were grown in sitting drops from a sample containing 0.6% labeled protein mixed with a solution consisting of 100 mM sodium acetate, 1 M diammonium hydrogen phosphate pH 4.5 (the scale bar is 0.2 mm in length). The images in (a) and (c) were obtained with white-light illumination. The images in (b) and (d) were obtained with a 520 nm light source and a low-pass filter at 550 nm (LP550).

in crystal growth, and the high success rate of MMS in this study was accompanied by a drastic decrease in the time required for crystal production. Consequently, seeding was systematically used in the following optimization experiments.

Out of the 34 hits obtained in the presence of seeds, several could be reproduced. The three best hits are displayed in Fig. 2. They corresponded to JBScreen JCSG++ conditions A8, B12 and E8 (Table 2) and yielded crystals that diffracted to 1.85, 2.09 and 1.80 Å resolution, respectively (Table 3). They all belonged to the same tetragonal space group and showed comparable unit-cell parameters. Refinement of the respective crystal structures is in progress and a complete analysis of the corresponding structures at high resolution will be published elsewhere.

To conclude, this work illustrates the usefulness of combining various crystallogeneses methods to efficiently define and optimize multiple crystallization conditions, and to ensure the production of well diffracting crystals. The availability of various growth conditions for *PhaCCA* crystals will also be an advantage for future soaking experiments with substrates (CTP, ATP and small RNAs).

Acknowledgements

The authors acknowledge the assistance of Guillaume Bec (IBMC–CNRS) from the UPR 9002 crystallization platform, as well as the following synchrotron facilities and associated scientists for beamtime provision for the project and assistance during data collection: the X06DA beamline at the Swiss Light Source, Villigen, Switzerland and PROXIMA-1 at the SOLEIL synchrotron, Saint-Aubin, France. They are grateful to the organizers and speakers of the Sixth FEBS Advanced Course on Macromolecular Crystallization (Czech Republic, June 2016), especially Terese Bergfors, Allan D’Arcy and Marc Pusey, for their advice regarding seeding and TFL methods.

Funding information

Funding for this research was provided by: LabEx NetRNA (grant No. ANR-10-LABX-0036_NETRNA); Labex Mitocross (grant No. ANR-11-LABX-0057_MITOCROSS); Ministère des Affaires Etrangères–Deutscher Akademischer Austauschdienst (grant No. 35317YM/57207407 PROCOPE

Hubert Curien 2016); Centre National de la Recherche Scientifique; Deutsche Forschungsgemeinschaft (grant No. MO 634/8-1); Université de Strasbourg (IDEX PhD grant).

References

- Adams, P. D., Afonine, P. V., Bunkóczi, G., Chen, V. B., Davis, I. W., Echols, N., Headd, J. J., Hung, L.-W., Kapral, G. J., Grosse-Kunstleve, R. W., McCoy, A. J., Moriarty, N. W., Oeffner, R., Read, R. J., Richardson, D. C., Richardson, J. S., Terwilliger, T. C. & Zwart, P. H. (2010). *Acta Cryst.* **D66**, 213–221.
- Bae, E. & Phillips, G. N. Jr (2004). *J. Biol. Chem.* **279**, 28202–28208.
- Bergfors, T. (2003). *J. Struct. Biol.* **142**, 66–76.
- Betat, H., Rammelt, C. & Mörl, M. (2010). *Cell. Mol. Life Sci.* **67**, 1447–1463.
- D’Arcy, A., Bergfors, T., Cowan-Jacob, S. W. & Marsh, M. (2014). *Acta Cryst.* **F70**, 1117–1126.
- D’Arcy, A., Villard, F. & Marsh, M. (2007). *Acta Cryst.* **D63**, 550–554.
- De Maayer, P., Anderson, D., Cary, C. & Cowan, D. A. (2014). *EMBO Rep.* **15**, 508–517.
- Ernst, F. G. M., Erber, L., Sammler, J., Jühling, F., Betat, H. & Mörl, M. (2018). *RNA Biol.* **15**, 144–155.
- Ernst, F. G. M., Rickert, C., Bluschke, A., Betat, H., Steinhoff, H. J. & Mörl, M. (2015). *RNA Biol.* **12**, 435–446.
- Kabsch, W. (2010). *Acta Cryst.* **D66**, 125–132.
- Karplus, P. A. & Diederichs, K. (2012). *Science*, **336**, 1030–1033.
- Li, F., Xiong, Y., Wang, J., Cho, H. D., Tomita, K., Weiner, A. M. & Steitz, T. A. (2002). *Cell*, **111**, 815–824.
- McCoy, A. J., Grosse-Kunstleve, R. W., Adams, P. D., Winn, M. D., Storoni, L. C. & Read, R. J. (2007). *J. Appl. Cryst.* **40**, 658–674.
- Mykytczuk, N. C. S., Wilhelm, R. C. & Whyte, L. G. (2012). *Int. J. Syst. Evol. Microbiol.* **62**, 1937–1944.
- Neuenfeldt, A., Just, A., Betat, H. & Mörl, M. (2008). *Proc. Natl Acad. Sci. USA*, **105**, 7953–7958.
- Newman, J. (2011). *Methods*, **55**, 73–80.
- Newman, J., Egan, D., Walter, T. S., Meged, R., Berry, I., Ben Jelloul, M., Sussman, J. L., Stuart, D. I. & Perrakis, A. (2005). *Acta Cryst.* **D61**, 1426–1431.
- Otálora, F., Gavira, J. A., Ng, J. D. & García-Ruiz, J. M. (2009). *Prog. Biophys. Mol. Biol.* **101**, 26–37.
- Pusey, M., Barcena, J., Morris, M., Singhal, A., Yuan, Q. & Ng, J. (2015). *Acta Cryst.* **F71**, 806–814.
- Tomita, K., Ishitani, R., Fukai, S. & Nureki, O. (2006). *Nature (London)*, **443**, 956–960.